Article

Extensive global wetland loss over the past three centuries

 Check for updates

Etienne Fluet-Chouinard[1,2,27] ✉, Benjamin D. Stocker[3,4,5,6], Zhen Zhang[7], Avni Malhotra[1], Joe R. Melton[8], Benjamin Poulter[9], Jed O. Kaplan[10], Kees Klein Goldewijk[11], Stefan Siebert[12,13], Tatiana Minayeva[14], Gustaf Hugelius[1,15,16], Hans Joosten[17,18], Alexandra Barthelmes[17,18], Catherine Prigent[19,20], Filipe Aires[19,20], Alison M. Hoyt[1], Nick Davidson[21,22], C. Max Finlayson[22,23], Bernhard Lehner[24], Robert B. Jackson[1,25] & Peter B. McIntyre[2,26]

Wetlands have long been drained for human use, thereby strongly affecting greenhouse gas fluxes, flood control, nutrient cycling and biodiversity[1,2]. Nevertheless, the global extent of natural wetland loss remains remarkably uncertain[3]. Here, we reconstruct the spatial distribution and timing of wetland loss through conversion to seven human land uses between 1700 and 2020, by combining national and subnational records of drainage and conversion with land-use maps and simulated wetland extents. We estimate that 3.4 million km² (confidence interval 2.9–3.8) of inland wetlands have been lost since 1700, primarily for conversion to croplands. This net loss of 21% (confidence interval 16–23%) of global wetland area is lower than that suggested previously by extrapolations of data disproportionately from high-loss regions. Wetland loss has been concentrated in Europe, the United States and China, and rapidly expanded during the mid-twentieth century. Our reconstruction elucidates the timing and land-use drivers of global wetland losses, providing an improved historical baseline to guide assessment of wetland loss impact on Earth system processes, conservation planning to protect remaining wetlands and prioritization of sites for wetland restoration[4].

Throughout most of human history, wetlands have been considered 'unproductive land' that is 'ripe for reclamation' for agriculture and urbanization[3]. Draining waterlogged soils has produced some of the most fertile agricultural lands on the planet[5]. Methods such as ditch construction and tile drainage date back millennia, and mechanization in the past century has further expedited wetland conversion[6]. Wetland drainage has also been pursued to prevent soil salinization or paludification (that is, peat formation)[5] to control vector-borne diseases[7], and to extract peat for fuel and soil amendments[8,9]. Together, the deliberate drainage of wetlands—plus impacts from climate change, rising sea levels, fires and groundwater extraction—have made wetlands among the most threatened ecosystems in the world[9].

Conserving wetland ecosystems has been recognized formally as an international priority since the 1971 Ramsar Convention, and was recently affirmed under Indicator 6.6.1 in the United Nations'

Sustainable Development Goals. These frameworks augment the 'no-net-loss' policies[10] erected in many nations that shifted away from the subsidy programmes encouraging wetland conversion to cropland during much of the twentieth century. A central rationale for modern wetland conservation policies is the economic value of the many ecosystem services they support[2,11]. Whereas rates of wetland conversion have declined in most countries, losses continue in some regions such as Indonesia, where tropical peat swamps have been drained for industrial plantations and smallholder agriculture until recently[12,13].

Accurate estimation of the extent, distribution and timing of wetland loss is essential to understand their effect on Earth system processes. Wetland losses affect terrestrial water storage[14], quality and supply[15], evapotranspiration[16], terrestrial-to-ocean carbon export[17], carbon balance[18], emissions of nitrous oxide[19] and methane[20], nutrient removal[21], flood regimes and groundwater recharge[22] and biodiversity[1,23].

[1]Department of Earth System Science, Stanford University, Stanford, CA, USA. [2]Center for Limnology, University of Wisconsin-Madison, Madison, WI, USA. [3]Department of Environmental Systems Science, ETH Zurich, Zürich, Switzerland. [4]Swiss Federal Institute for Forest, Snow and Landscape Research WSL, Birmensdorf, Switzerland. [5]Institute of Geography, University of Bern, Bern, Switzerland. [6]Oeschger Centre for Climate Change Research, University of Bern, Bern, Switzerland. [7]Earth System Science Interdisciplinary Center, University of Maryland, College Park, MD, USA. [8]Climate Research Division, Environment and Climate Change Canada, Victoria, British Columbia, Canada. [9]NASA Goddard Space Flight Center, Biospheric Sciences Laboratory, Greenbelt, MD, USA. [10]Department of Earth Sciences, The University of Hong Kong, Hong Kong SAR, China. [11]Faculty of Geosciences, Copernicus Institute of Sustainable Development, Utrecht University, Utrecht, The Netherlands. [12]Department of Crop Sciences, Georg-August-Universität Göttingen, Goettingen, Germany. [13]Centre of Biodiversity and Sustainable Land Use, University of Göttingen, Göttingen, Germany. [14]Care for Ecosystems, Goerlitz, Germany. [15]Department of Physical Geography, Stockholm University, Stockholm, Sweden. [16]Bolin Centre for Climate Research, Stockholm University, Stockholm, Sweden. [17]Faculty of Mathematics and Natural Sciences, Peatland Studies and Paleoecology, University of Greifswald, Greifswald, Germany. [18]Greifswald Mire Centre, Greifswald, Germany. [19]Sorbonne Université, Observatoire de Paris, Université PSL, CNRS, LERMA, Paris, France. [20]Estellus, Paris, France. [21]Nick Davidson Environmental, Queens House, Wigmore, UK. [22]Gulbali Institute for Land, Water and Society, Charles Sturt University, Elizabeth Mitchell Drive, Albury, New South Wales, Australia. [23]IHE Delft, Institute for Water Education, Delft, The Netherlands. [24]Department of Geography, McGill University, Montreal, Quebec, Canada. [25]Woods Institute for the Environment and Precourt Institute for Energy, Stanford University, Stanford, CA, USA. [26]Department of Natural Resources and the Environment, Cornell University, Ithaca, NY, USA. [27]Present address: Institute for Atmospheric and Climate Science, ETH Zurich, Zurich, Switzerland. ✉e-mail: efluet@stanford.edu
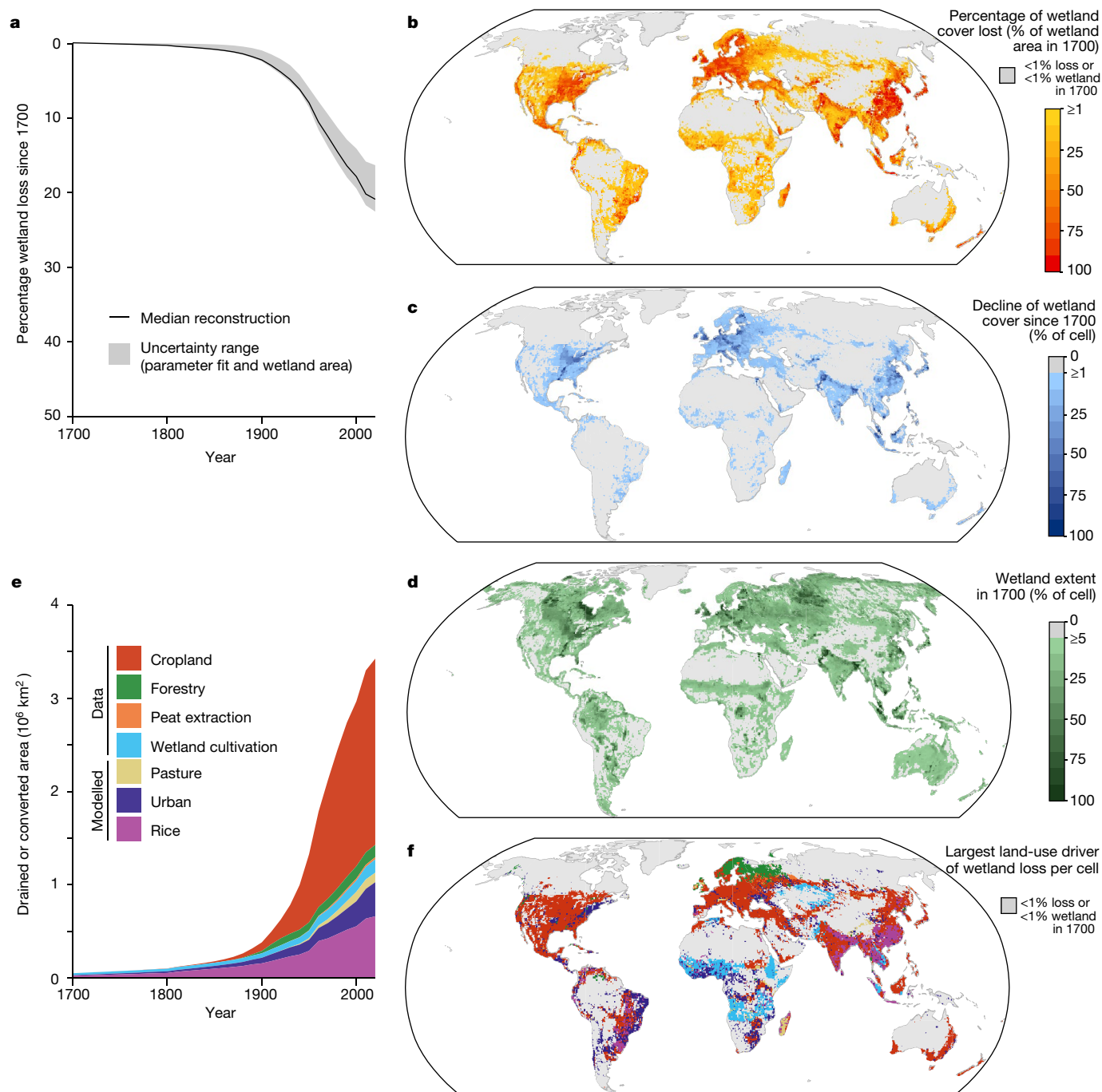
Fig. 1 | Reconstructed extent of drained, lost or converted wetlands between 1700 and 2020 globally. a, The percentage of global wetland area lost was modest before 1900 but has since accelerated. The uncertainty band (grey) is derived from the ensemble of permutations of parameters and wetland maps used to calculate wetland loss (Methods). **b**, Map of cumulative percentage wetland loss as a fraction of wetland cover in 1700. **c**, Map of the extent of wetland decline, calculated as difference in wetland cover between 1700 and 2020. **d**, Map of natural wetland extent in 1700. **e**, Cumulative drivers of wetland loss by land-use class to 2020; cropland and rice cultivation are the primary uses of converted wetlands worldwide. **f**, Map of dominant land use for converted wetlands, following legend of **e**. See Supplementary Fig. 5 for individual land-use maps.

Moreover, the environmental legacy of wetland drainage can last for centuries, thereby complicating the accounting of their cumulative impact, particularly for past greenhouse gas emissions arising from historical conversions[24]. Degradation of peatlands, a wetland type characterized by organic soil horizons of over 40 cm, is particularly impactful due to their major role in soil carbon storage[25,26]. Unlike other major land-use transformations, such as deforestation or irrigation, wetland conversion has yet to be reconstructed globally at the temporal and spatial resolution required for Earth system simulations[27].

High estimates of wetland loss have been reported in the literature for decades[1,28,29]—for example, "50% of the world's wetlands have been lost since 1900" (refs. [1,30]). More recent estimates, based on regional extrapolations[3,31] and geospatial overlay approaches[16,32], have ranged between 28 and 87% net losses since 1700. These disparities undermine the credibility of broad comparisons with loss rates of other ecosystem types—for example, forests[28,29]. A rigorous estimation of wetland loss has been hindered by the paucity of historical data, requiring the unification of data and modelling approaches.
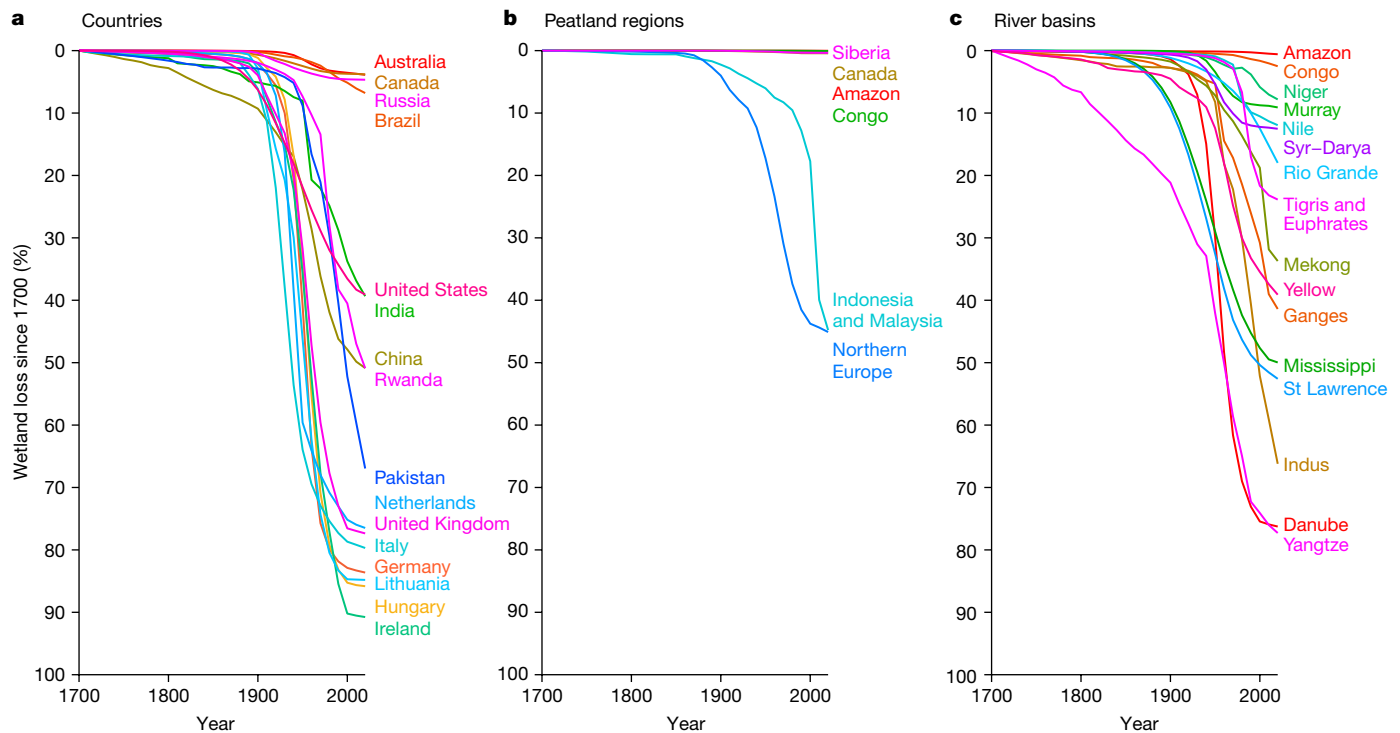
Fig. 2 | Heterogeneous wetland loss across countries, peatland regions and river basins of the world. a–c, Percentage of wetland loss since the 1700 baseline within selected countries (**a**), peatland-dense regions (**b**; see peatland regions in Supplementary Fig. 7) and major river basins (**c**) (Regional summary of wetland loss).

Here, we use a two-step approach to estimate the conversion of wetlands to seven classes of human land use between 1700 and 2020 (Supplementary Fig. 1 and Methods). Our analysis focuses on inland wetlands—which we define as any area inundated or waterlogged for at least one continuous month during the period of record, regardless of surface vegetation—but excludes permanently inundated areas (river channels and lakes), coastal intertidal zones and near-shore marine wetlands. First, we compiled a database of 3,320 national and sub-national drainage and land-use records, on area converted and peat mass extracted, from 154 countries and across four land uses (cropland, forestry, peat extraction and wetland cultivation; Supplementary Figs. 2–4). We interpolated country-level drainage records into continuous time series, then spatially distributed the drained area in proportion to the joint probability of each of the four land uses and the potential wetland cover fractions in each 0.5° grid cell globally. Second, we supplemented national statistics by modelling three additional land-use classes that also cause wetland conversion (irrigated rice, pasture and urban areas), which were calibrated to maximize agreement with 121 geolocated independent regional estimates of percentage wetland area change. This approach unifies the main available information sources on wetland loss to produce a comprehensive, data-driven estimate at the global scale.

Global drivers of wetland loss

We estimate that the global area of natural wetlands has declined by 3.4 million km² (confidence interval (CI) 2.9–3.8 Mkm²) since 1700 (Fig. 1a–c). This estimate corresponds to a loss of 21% (CI 16–23%) of the 15.8 Mkm² (CI 13.6–17.5 Mkm²) of wetlands estimated to have existed in 1700 (Fig. 1d). We label the total area affected by conversion to these seven land uses as 'wetland loss', although we recognize that they vary in severity of impacts, ranging along a gradient from full drainage and replacement of natural wetland (for example, upland cropland, forestry, urban areas and pasture), to drainage and soil degradation

(for example, peat extraction) to conversion to artificial wetlands with controlled water levels (for example, irrigated rice and wetland cultivation).

Wetland drainage for upland croplands was the most common cause of loss of natural wetlands (2.0 Mkm²; 61.7% of total loss), followed by conversion to flooded rice (18.2%), urban areas (8.0%), forestry (4.7%), wetland cultivation (4.3%), pasture (2.0%) and peat extraction (0.9%; Fig. 1e). Despite its limited global importance, forestry was the dominant driver of wetland loss in Sweden, Finland and Estonia, accounting for over 45% of total losses in these countries (Fig. 1f). We estimate that 792 million tonnes of dry peat have been extracted since 1700 for fuel or fertilizer, leading to the degradation of 0.026 Mkm² of peatlands. Peatland degradation was concentrated primarily in Ireland, Northern Europe and Western Russia. Conversion to flooded rice or other wetland cultivation systems is another regionally important driver of loss, particularly in Asia and SubSaharan Africa, where they account for around 40% of all losses[33].

The highest global rates of wetland area loss (0.46 Mkm² yr⁻¹ or 2.2% yr⁻¹) occurred in the 1950s when government programmes subsidized drainage for agriculture and forestry across North America, Europe and China[34] (Fig. 1a and Supplementary Fig. 6). However, the scarcity of drainage records before 1850 could lead to an underestimation of losses in countries with known early drainage or peat extraction. Thus, our estimates of both long-term trends and cumulative losses may be underestimated if early wetland conversions were not recorded in later surveys.

Regional hotspots of loss

Regional hotspots, where over 50% of wetlands were lost between 1700 and 2020, are found in the United States, Europe, Central Asia, India, China, Japan and Southeast Asia (Figs. 1b and 2a). Although we find no justification for the generalization that "more than half of the world's wetlands have been lost"[1], several nations do exceed that threshold
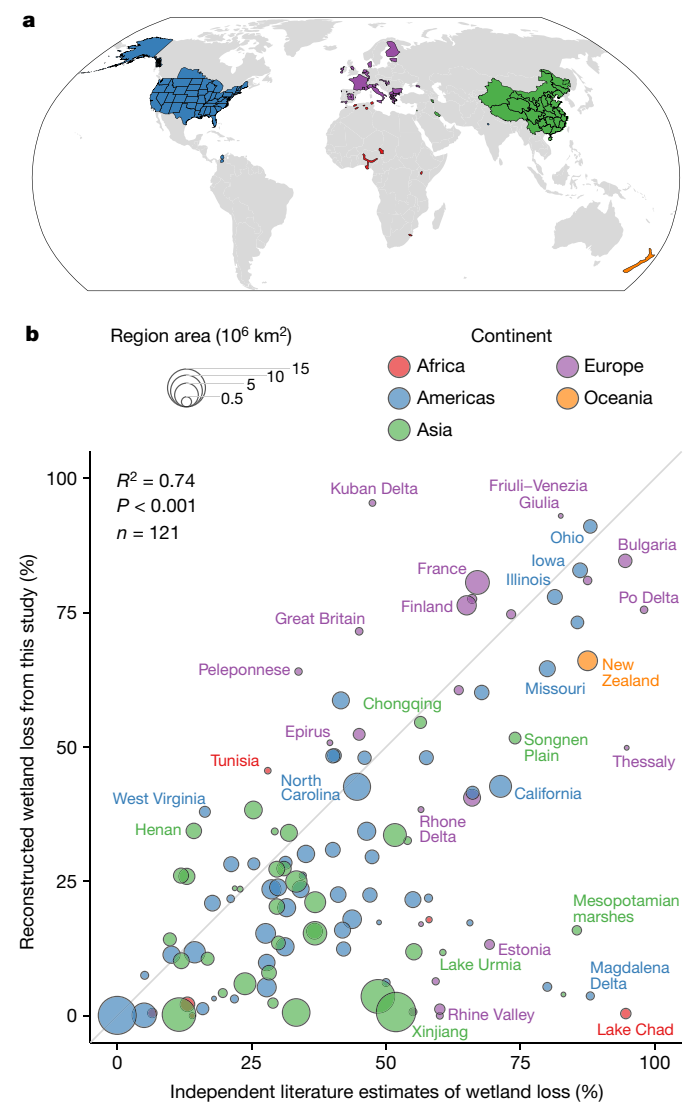
Fig. 3 | Regional estimates of wetland loss to calibrate our reconstruction.
a, Areas covered by 121 regional wetland loss estimates (see key in **b** for coloration by continent) compiled from independent databases. **b**, Comparison of our reconstructed wetland losses (*y* axis) with reported regional losses (*x* axis) indicates high overall agreement, particularly in regional hotspots of conversion. Region area (circle size) was used as a weighting term for calibration of our reconstruction to regional estimates, showing that the most discrepant regions cover smaller areas.

(Supplementary Table 1). Just five countries account for over 40% of all global wetland losses: United States (15.6% of total), China (12.6%), India (6.5%), Russia (4.5%) and Indonesia (4.1%).

We estimate that 0.51 Mkm^2 (11%) of peatlands have been lost when accounting for all seven land-use classes. This figure is similar to the 0.5 M km^2 peatland loss estimated previously by land-use overlays[35]. Among peatland-rich regions, Northern European peatlands have undergone the earliest and highest losses since 1700, followed by a recent increase of peatland drainage in Indonesia and Malaysia for oil palm cultivation (Fig. 2b). Peatland losses in Indonesia and Malaysia are underestimated by our reconstruction, even if guided by regional data indicating high peatland loss[13], because our reconstruction method conflates all wetland types when allocating drainage to both peatland and non-peatland areas. By contrast, the vast northern peatlands of Siberia and Canada have been largely spared from human conversion to date, but our estimates exclude regionally important mining and oil extraction[36]. Draining peatlands merits special attention due to release

of soil organic carbon accumulated over millennia under low-redox conditions as greenhouse gases to the atmosphere[18,25].

Among the world's major river basins, most wetland losses occurred in populated temperate watersheds such as the Danube, Indus, Yangtze and Mississippi rivers (Fig. 2c). Substantial wetland loss across river basins can lead to increased flooding[37] and degraded water quality[15,38]. These impacts are also caused by the loss of geographically isolated wetlands, which rarely benefit from the same protection as those connected to navigable waters[39]. To date, some tropical river basins such as the Amazon and Congo have retained most of their riparian wetlands, thereby protecting the role of their lateral river–floodplain connectivity for ecosystem productivity and carbon export[40].

Calibration to regional data

We reconciled drainage statistics and wetland loss data in many regions, ensuring that our global approach aligns with the best available regional estimates of wetland loss. Specifically, we modelled losses to three key classes of land use (irrigated rice, pastures and urban areas) based on 121 geolocated regional estimates of percentage wetland conversion (Fig. 3a). These regional estimates, derived from soil maps and local records, are the closest available proxies to direct measurements of historic wetland area and change (Methods). Following calibration and fitting, our reconstruction achieved reasonable agreement with these independent estimates (Fig. 3b; R^2 ensemble range, 0.62–0.74), and successfully identified most known hotspots of wetland loss.

Discrepancies with global loss estimates

The patchiness of available historical data on wetland drainage and our restrained imputation over data gaps probably led to our loss estimates being conservative, as illustrated by the negative bias (−14 to −23%; Fig. 3b), indicating modest underestimation by our reconstruction relative to regional data. Nevertheless, the magnitude of this mismatch is far less than the disparity between our global wetland loss estimate and previous findings from meta-analyses (Fig. 4). Published extrapolations of regional estimates of annual wetland change (percentage yr^{-1}) data put global losses as high as 87% since 1700 (ref. [3]) and 35% since 1970 (ref. [31]). These extrapolations are based on historic records and land-use and soil maps which, even if they were locally accurate, are unlikely to be representative of wetland heterogeneity across the globe[3,31]. Indeed, comparing the statistical distribution of regional loss rates with that of all grid cells in our reconstruction suggests a strong bias of regional studies toward high-loss areas (two-tailed Kolmogorov–Smirnov test, $D = 0.48$–0.61, $P < 0.0001$; Supplementary Fig. 8), probably causing overestimation of global wetland losses. Our exclusion of marine wetlands (for example, mangroves), which are included in other global estimates (Fig. 4), is unlikely to explain the overall disparity because marine wetlands are modest in aggregate area relative to inland wetlands[3].

The geography of wetland losses indicated by our global reconstruction also contrasts with previous spatial analyses. Geospatial overlays of cropland and urban land-use maps on an idealized potential wetland cover suggest cumulative conversion of 28–33% (refs. [16,25,32]), which is roughly comparable to our reconstruction (Fig. 4). However, some geospatial overlay estimates[32] differ sharply in geographic distribution from our reconstruction, particularly in suggesting greater losses in South America (Supplementary Table 2). The large uncertainty of their spatial patterns reflects disagreement between underlying land use and potential wetland extents[41], as well as differing interpretations of their spatial overlap[18].

Although our reconstruction probably underestimates wetland loss since 1700 in some regions, global cumulative losses are unlikely to be severely underestimated for several reasons. First, our reconstruction captures the largest centres of drainage across North America,
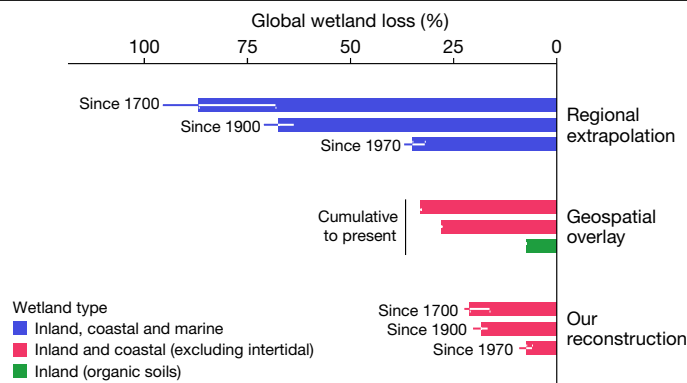
Fig. 4 | Global wetland loss estimates from the literature and our study diverge markedly, with our reconstructed losses being lower than most previous estimates. The highest losses are estimated by meta-analyses extrapolating regional records of percentage loss. Geospatial overlays generate percentage loss estimates similar to our reconstruction, but some diverge in their starting baseline and geographic distribution of loss. Sources also vary in the drivers included (meta-analysis includes mining, overgrazing and so on; geospatial overlays include only cropland and urban), and have their own respective wetland type definitions (for example, coastal). Each bar represents an individual estimate and each error bar represents its respective uncertainty range. See Supplementary Table 3 for sources.

Europe and Asia, and those regions with data gaps are insufficient to substantially increase the estimated global loss. Second, we probably overestimated loss in arid regions where drainage (for example, Pakistan) is installed to prevent soil salinization from irrigation but is interpreted as wetland loss by our method[42]. Third, among our ensemble of reconstructions using different wetland maps, global estimates all converged on similar percentage losses because the higher wetland area from some maps was offset by higher wetland area losses (Supplementary Fig. 9).

Resolving the recent declines in wetland area is essential for evaluation of progress toward Sustainable Development Goal (SDG) 6.6.1: change in the extent of water-related ecosystems over time, and our reconstruction fills an important knowledge gap. Indeed, SDG 6.6.1 benchmarks wetland loss against a 1970 baseline, and the gap between our reconstruction and extrapolated rates of loss is magnified during this recent period. However, comparing our long-term reconstruction and regional extrapolations since 1970 (ref. [31]) suggests that even increased density of the monitoring network has not overcome biases arising from reliance on high-loss sites and a shifted baseline (two-tailed Kolmogorov–Smirnov test, $D = 0.31$–0.46, $P < 0.0001$; Supplementary Fig. 8). In the future, it will be important to expand monitoring in ways that diminish biases in the network of sites used to represent global dynamics of wetland losses.

Conclusions

Our reconstruction of three centuries of wetland conversion draws on both drainage statistics and regional loss estimates to produce a temporally explicit trajectory of global wetland extent. These results show that most previous studies overestimated global wetland conversion, by relying on data concentrated in high-loss regions. However, our findings should not lessen the urgency to protect and restore wetland ecosystems, particularly in regions with ongoing rapid drainage, as well as remnants located in high-loss regions.

Our maps of wetland extent, conversion rates and land-use drivers enable numerous applications. This information provides a baseline for conservation targets and prioritization of the protection of wetland types and dependent species. In a restoration context, understanding land-use histories helps choose sites for interventions such as rewetting to reduce radiative forcing or enhance nutrient removal[4]. For Earth system modelling, the extent of wetland conversion is essential to quantify the full anthropogenic impact on carbon and water budgets[17,20]. Because the world's wetlands face further pressures in the coming decades, extending our reconstruction with continuous monitoring of wetland cover via remote sensing[43], national reporting and networks of sites is urgently needed.

Online content

Any methods, additional references, Nature Portfolio reporting summaries, source data, extended data, supplementary information, acknowledgements, peer review information; details of author contributions and competing interests; and statements of data and code availability are available at https://doi.org/10.1038/s41586-022-05572-6.

1. Zedler, J. B. & Kercher, S. Wetland resources: status, trends, ecosystem services, and restorability. *Annu. Rev. Environ. Resour.* **30**, 39–74 (2005).
2. Finlayson, C. M. et al. *Millennium Ecosystem Assessment: Ecosystems and Human Well-being: Wetlands and Water Synthesis* (World Resources Institute, 2005).
3. Davidson, N. C. How much wetland has the world lost? Long-term and recent trends in global wetland area. *Mar. Freshwater Res.* **65**, 934 (2014).
4. Günther, A. et al. Prompt rewetting of drained peatlands reduces climate warming despite methane emissions. *Nat. Commun.* **11**, 1644 (2020).
5. Schultz, B., Thatte, C. D. & Labhsetwar, V. K. Irrigation and drainage. Main contributors to global food production. *Irrig. Drain.* **54**, 263–278 (2005).
6. Valipour, M. et al. The evolution of agricultural drainage from the earliest times to the present. *Sustainability* **12**, 416 (2020).
7. Holden, J., Chapman, P. J. & Labadz, J. C. Artificial drainage of peatlands: hydrological and hydrochemical process and wetland restoration. *Prog. Phys. Geogr.* **28**, 95–123 (2004).
8. Joosten, H. & Clarke, D. *Wise Use of Mires and Peatlands* (International Mire Conservation Group and International Peat Society, 2002).
9. van Asselen, S., Verburg, P. H., Vermaat, J. E. & Janse, J. H. Drivers of wetland conversion: a global meta-analysis. *PLoS ONE* **8**, e81292 (2013).
10. Maron, M. et al. The many meanings of no net loss in environmental policy. *Nat. Sustain.* **1**, 19–27 (2018).
11. Costanza, R. et al. The value of the world's ecosystem services and natural capital. *Nature* **387**, 253–260 (1997).
12. Page, S. E. & Hooijer, A. In the line of fire: the peatlands of Southeast Asia. *Philos. Trans. R. Soc. Lond. B Biol. Sci.* **371**, 20150176 (2016).
13. Miettinen, J., Shi, C. & Liew, S. C. Land cover distribution in the peatlands of Peninsular Malaysia, Sumatra and Borneo in 2015 with changes since 1990. *Glob. Ecol. Conserv.* **6**, 67–78 (2016).
14. Wada, Y. et al. Recent changes in land water storage and its contribution to sea level variations. *Surv. Geophys.* **38**, 131–152 (2017).
15. Xu, J., Morris, P. J., Liu, J. & Holden, J. Hotspots of peatland-derived potable water use identified by global analysis. *Nat. Sustain.* **1**, 246–253 (2018).
16. Sterling, S. M., Ducharne, A. & Polcher, J. The impact of global land-cover change on the terrestrial water cycle. *Nat. Clim. Change* **3**, 385–390 (2013).
17. Abril, G. & Borges, A. V. Ideas and perspectives: carbon leaks from flooded land: do we need to replumb the inland water active pipe? *Biogeosciences* **16**, 769–784 (2019).
18. Qiu, C, et al. Large historical carbon emissions from cultivated northern peatlands. *Sci. Adv.* **7**, eabf1332 (2021).
19. Bahram, M. et al. Structure and function of the soil microbiome underlying N₂O emissions from global wetlands. *Nat. Commun.* **13**, 1430 (2022).
20. Paudel, R., Mahowald, N. M., Hess, P. G. M., Meng, L. & Riley, W. J. Attribution of changes in global wetland methane emissions from pre-industrial to present using CLM4.5-BGC. *Environ. Res. Lett.* **11**, 034020 (2016).
21. Cheng, F. Y., Van Meter, K. J., Byrnes, D. K. & Basu, N. B. Maximizing US nitrate removal through wetland protection and restoration. *Nature* **588**, 625–630 (2020).
22. Bullock, A. & Acreman, M. The role of wetlands in the hydrological cycle. *Hydrol. Earth Syst. Sci.* **7**, 358–389 (2003).
23. Castellano, M. J., Archontoulis, S. V., Helmers, M. J., Poffenbarger, H. J. & Six, J. Sustainable intensification of agricultural drainage. *Nat. Sustain.* **2**, 914–921 (2019).
24. IPCC. *2013 Supplement to the 2006 IPCC Guidelines for National Greenhouse Gas Inventories: Wetlands: Methodological Guidance on Lands with Wet and Drained Soils, and Constructed Wetlands for Wastewater Treatment* (2013).
25. Tubiello, F., Biancalani, R., Salvatore, M., Rossi, S. & Conchedda, G. A worldwide assessment of greenhouse gas emissions from drained organic soils. *Sustainability* **8**, 371 (2016).
26. Hugelius, G. et al. Large stocks of peatland carbon and nitrogen are vulnerable to permafrost thaw. *Proc. Natl Acad. Sci. USA* **117**, 20438–20446 (2020).
27. Pongratz, J. et al. Models meet data: challenges and opportunities in implementing land management in Earth system models. *Glob. Chang. Biol.* **24**, 1470–1487 (2018).
28. Intergovernmental Science-Policy Platform on Biodiversity and Ecosystem Services. *Land Degradation Assessment* (2018).
29. Ramsar Convention Secretariat, Ramsar Convention on Wetlands. *Global Wetland Outlook: State of the World's Wetlands and their Services to People* (2018).
30. Winkler, M. G. & DeWitt, C. B. Environmental impacts of peat mining in the United States: documentation for wetland conservation. *Environ. Conserv.* **12**, 317–330 (1985).

Article

31. Darrah, S. E. et al. Improvements to the Wetland Extent Trends (WET) index as a tool for monitoring natural and human-made wetlands. *Ecol. Indic.* **99**, 294–298 (2019).
32. Hu, S., Niu, Z., Chen, Y., Li, L. & Zhang, H. Global wetlands: potential distribution, wetland loss, and status. *Sci. Total Environ.* **586**, 319–327 (2017).
33. Verhoeven, J. T. A. & Setter, T. L. Agricultural use of wetlands: opportunities and limitations. *Ann. Bot.* **105**, 155–163 (2010).
34. Pavelis, G. A. *Farm Drainage in the United States: History, Status, and Prospects* (Economic Research Service, 1987).
35. Leifeld, J. & Menichetti, L. The underappreciated potential of peatlands in global climate change mitigation strategies. *Nat. Commun.* **9**, 1071 (2018).
36. Rooney, R. C., Bayley, S. E. & Schindler, D. W. Oil sands mining and reclamation cause massive loss of peatland and stored carbon. *Proc. Natl Acad. Sci. USA* **109**, 4933–4937 (2012).
37. Acreman, M. & Holden, J. How wetlands affect floods. *Wetlands* **33**, 773–786 (2013).
38. Creed, I. F. et al. Enhancing protection for vulnerable waters. *Nat. Geosci.* **10**, 809–815 (2017).
39. Cohen, M. J. et al. Do geographically isolated wetlands influence landscape functions? *Proc. Natl Acad. Sci. USA* **113**, 1978–1986 (2016).
40. Borges, A. V. et al. Divergent biophysical controls of aquatic CO_2 and CH_4 in the World's two largest rivers. *Sci. Rep.* **5**, 15614 (2015).
41. Melton, J. R. et al. Present state of global wetland extent and wetland methane modelling: conclusions from a model inter-comparison project (WETCHIMP). *Biogeosciences* **10**, 753–788 (2013).
42. Ritzema, H. P. Drain for gain: managing salinity in irrigated lands—a review. *Agric. Water Manage.* **176**, 18–28 (2016).
43. Gallant, A. The challenges of remote monitoring of wetlands. *Remote Sens.* **7**, 10938–10950 (2015).

Methods

Methodological overview

We used five primary data sources to produce a gridded reconstruction of wetland loss: (1) national and subnational statistics reporting wetland area drained or converted, (2) regional data on percentage wetland loss, (3) present-day wetland maps, (4) simulated wetland maps and (5) reconstructed land-use maps. Our methodology combines all input data to produce a globally gridded reconstruction of wetland drainage, conversion and degradation over the period 1700–2020.

Our approach to reconstruction of global wetland loss consists of four steps (see Supplementary Fig. 1 for a schematic summarizing methods). National statistics for four land-use drivers (cropland, forestry, peat extraction and wetland cultivation) were first interpolated into continuous time series (at 10 year intervals, the time step of the analysis). Second, potential wetland area was generated from maps of present-day wetlands and simulations of idealized wetland cover. The national drainage time series were then mapped on a 0.5° grid based on the geographic distribution of land use and potential wetland. This mapping was conducted simultaneously with three additional land uses (irrigated rice, pasture and urban areas) whose land-use conversion was modelled based on potential wetland and land-use maps. Fourth, once land-use drainage and conversion had been mapped, the resulting wetland loss was compared against 121 independent regional estimates of percentage wetland loss. The last two steps of mapping and comparison were repeated through an optimization process until optimal parameter values maximizing agreement were found.

Our reconstruction model focuses on long-term wetland losses and therefore does not represent wetland gains resulting from drainage disrepair, land-use abandonment or wetland restoration. We use 'wetland loss' as a catch-all term for 'drainage, conversion, degradation or regulation', and our global figures on wetland loss should not be understood as causing a similar decline in ecosystem function across the world.

Wetland definition

We define the inland and coastal wetlands included in our analysis based on a methodological rather than an a priori definition or typology. Our operational wetland definition is inherited from wetland maps we used that represent wetlands on land and above the maximum tideline. These maps (described below) represent areas that are inundated or waterlogged, vegetated or not (for example, forested swamps, bare floodplains) from which we removed open water ecosystems (for example, rivers, reservoirs and lakes), rice paddies and the annual maximum water extent along coastlines. As a result, intertidal and near-shore marine wetlands (for example, unvegetated tidal flats, salt marshes, mangroves and seagrasses) are excluded but coastal wetlands above the tideline remain (for example, deltas). Wetlands are land inundated or saturated by water intermittently, periodically or seasonally, because we used a minimum period of inundation or saturation of 1 month over the respective observation periods (13–15 years) for an area to be considered a wetland. This maximalist definition is used to balance the known gaps in wetland maps for small wetlands and below dense canopy.

Input data

National drained area statistics. Data on areas artificially drained or cultivated in wetlands, as well as the volume of peat extracted, have been collected by state agencies for decades as part of agricultural or economic surveys. We compiled 3,320 national and subnational records of the areas drained or wetlands converted to different land uses (Supplementary Fig. 2). We classified national-scale data ($n = 1,949$) into four land uses: cropland ($n = 396$, 20.3% of national data count), forestry ($n = 58$, 3.0%), peat extraction ($n = 1,291$; 66.2%) and wetland cultivation ($n = 204$, 10.5%; Supplementary Fig. 3). Subnational data ($n = 1,371$) were similarly organized into four land uses but with different relative shares of land-use drivers: cropland ($n = 1,020$, 74.4% of subnational total),

forestry ($n = 57$, 4.2%), peat extraction ($n = 284$; 20.7%) and wetland cultivation ($n = 10$, 0.7%; Supplementary Fig. 4). The database covers 154 countries and is concentrated in the post-1950 period (average and standard deviation; national: 1977 ± 32; subnational: 1981 ± 53; Supplementary Figs. 10 and 11). Documentation of wetland conversion before 1900 is sparse. We chose the baseline of 1700 to capture the time period before national drainage statistics were first recorded, allowing us to assume that the entire drained wetland area included in national and subnational statistics was drained after 1700. We acknowledge that drainage is known to have emerged before 1700 in several places—for example, for agriculture in Egypt, Mesopotamia, India and China[6] and for peat extraction in the Netherlands[44]. This early drainage affects the baseline of our relative wetland loss quantification, but not our absolute area estimates. Refining estimates of early losses and pre-1700 wetland extent will probably require new palaeo-ecological data such as pollen and sediment records[45].

Cropland drainage statistics were compiled from existing databases and publications, mainly from Pavelis[34], Feick et al.[46], the International Commission on Irrigation and Drainage[47] and the Food and Agriculture Organization (FAO)[48]. We also compiled data on the start year of subsidy programmes for the formation of drainage districts in the United States to constrain the temporal model of drainage. We assumed that drainage was negligible before the start of subsidies because, nearly everywhere, data on drained areas become available only decades after the recorded initiation of drainage projects. This assumption is adequate for regions for which data collection coincided with state-sponsored reclamation projects (for example, states affected by the Swamp and Overflowed Lands Act of 1850 (refs. [34,49])). We used a ranking of data sources from manual interpretation to resolve conflicting data for the same countries and time periods that may originate from differences in drainage or land-use definitions, generally selecting larger areas from more encompassing definitions.

For wetland cultivation, we compiled data from the FAO's AQUASTAT[50] on area cultivated under the following practices: lowland cultivation, flood recession agriculture and spate irrigation. Wetland cultivation practices were separated from other drainage types because they maintain wet or inundated conditions during part of the year and thus do not functionally replace wetland ecosystems. Nevertheless, we consider this transition to management by humans as a loss of the natural wetland ecosystem. Despite our attempt to treat land-use classes as mutually exclusive in our methodology, some double counting is possible between cropland, irrigated rice and wetland cultivation in regions in which data definitions overlap and are challenging to resolve.

For peat extraction, we collected data on dry peat mass extracted annually (tonnes per year; excluding briquettes and other processed fuels) as well as on the area of peatland drained for extraction. Peat mass and area were combined in a cumulative time series (Drained area time series hindcasting). The rise and decline in annual peat extraction rates during the twentieth century could be captured for certain countries whereas for others the compiled data represented only their decline, although earlier peat extraction industries are documented (for example, the Netherlands[44] and Ireland[51]), leading to a probable underestimation of the oldest peat drainage.

Despite being the most common method of wetland reclamation, installation of surface or subsurface drainage can also occur outside of wetlands. Artificial drainage can be installed in upland areas to prevent salinization and paludification, or to improve growing conditions[42,52]. National statistics rarely specify the objective of drainage, preventing us from distinguishing between drainage leading to wetland loss and otherwise. However, in temperate, humid and semihumid climatic zones, where most drainage records originate, drainage is primarily designed for reclamation of wet and waterlogged lands[52].

Regional data on wetland fraction lost. Regional estimates of wetland area or their fraction lost have been reported across the world

from a variety of approaches: land and soil surveys, land-use conversion records, historic hydric soils maps and remote sensing. Such data provide the best available benchmark and calibration target for our reconstruction. We compiled estimates from four data sources[3,31,53,54]: most data originate from country-wide assessments for the United States (1780–1980 (ref. [54])) and China (1978–2008 (ref. [53])). We then filtered these data using four screening criteria to retain only those records that (1) include inland wetlands, and not exclusively coastal or man-made wetlands, (2) cover an area over 10,000 km[2], (3) span a time period of at least 30 years and (4) provide both a start and end year. Application of these criteria ensured that those regions would provide a comparison at scales detectable by the reconstruction. We then geographically delineated 121 non-overlapping regions (Fig. 3a) for which available data met these criteria and consulted the original sources for maps or descriptions wherever possible. Some regional estimates are probably geographic extrapolations from smaller local estimates within those regions. The resulting 121 regional estimates collectively cover 16% of the world's land mass, occupying 190,000 km[2] on average (s.d. 280,000 km[2]) and span an average of 125 years (s.d. 87.6 years).

Present-day wetland cover. Present-day wetland area distributions were taken from three sources: WAD2M (13.8 Mkm[2])[55] and GIEMS v.2.0 (ref.[56]) (12.5 Mkm[2]), produced from multisensor remote sensing, and GLWD (10.9 Mkm[2]), compiled from a selection of maps and charts[57], provided in original resolutions of 0.25°, 0.25° and 0.0083° (30 arc-second), respectively. Several preprocessing steps were required to produce three comparable static wetland maps. First, we calculated the maximum inundated area fraction for each grid cell from the WAD2M and GIEMS v.2 monthly time series. Second, we processed GIEMS v.2 following the method previously used to generate WAD2M[55] to retain only vegetated wetlands: subtract the area fraction of open water bodies[58], ocean water cover[59] and irrigated rice area[60] within 0.5° grid cells, but retain a minimum wetland fraction from wetland maps that represent saturated soils rather than inundation[61,62]. The exclusion of ocean water cover at high tide leads our reconstruction to include inland and coastal wetland but exclude off-shore marine wetlands. Third, GLWD classes 4–12 were selected to include only vegetated wetland classes (excluding rivers, lakes and reservoirs) and aggregated to 0.5° grid cells. As a result, the three wetland maps represent the maximum extent of seasonally inundated or water-saturated land areas, excluding open water bodies, rice paddies and off-shore marine wetlands. Our three wetland maps diverge in both the extent of global wetland area by 2.9 Mkm[2] (10.9–13.8 km[2]; 23% of the average) and their geographic distribution (Supplementary Fig. 12). The differences in time period covered—2000–2018 for WAD2M, 1992–2015 for GIEMS v.2 and 1970s–1990s for GLWD—are unlikely to be a major source of disagreement in regard to the global wetland area.

Simulated wetland cover. We used the cell-wise maximum simulated wetland area fraction from grids of simulated monthly time series to inform the spatial mapping of drainage statistics, and to estimate the extent of losses from the three modelled land uses (irrigated rice, pasture and urban areas). We used four simulated wetland cover datasets from four land surface models: ORCHIDEE, SDGVM and DLEM, compiled for a multimodel intercomparison project[41], and from LPJ-wsl[63] (Supplementary Fig. 13). Each model dynamically simulates wetland extent as the fraction of the inundated area in each grid cell, using subgrid-scale topography information and following a TOPMODEL approach[64]. The water table is simulated in response to soil type, runoff and local water balance. These models do not simulate surface hydrodynamics, and hence probably underestimate the area of riverine floodplains and coastal wetlands. Importantly, simulations exclude the direct impact of human land use as a driver of wetland loss, and thus represent areas where wetlands should naturally form. The simulated wetland area of all models represents the period 1993–2004 and was generated

from transient model simulations forced over the period 1932–2009 (ref. [65]). We took the grid cell maximum over 1993–2004 for each model and used the four resulting static simulated wetland cover data for 1700–2020, thereby ignoring any climate-driven change in wetland area and distribution since 1700. Among models, the range of simulated global natural wetland extents is wide (12.0–64.6 Mkm[2]) and much larger than fluctuations over time within individual models. This led us to use these data only to inform the spatial distribution of wetland conversion rather than its overall magnitude. All maps were resampled to a grid cell resolution of 0.5° before calculations.

Reconstructed land-use maps. We used gridded historical land-use estimates to inform the spatial allocation of drainage data, as well as help determine the extent of wetland losses from the three modelled land uses (irrigated rice, pasture and urban areas). We used the land-use maps from HYDE 3.2 (ref. [66]) to represent cropland, pasture, irrigated rice and urban areas since 1700. The area occupied by each land use is estimated in HYDE 3.2 from population hindcasts and assumed per capita land-use requirements[67]. Cropland area (upland seasonal and perennial crops) was used to map both conversion to croplands and wetland cultivation (their respective areas from national records were mapped sequentially), whereas other wetland loss drivers were matched one-to-one with their respective land use. Data on forest area (primary and secondary forests) affected by wood extraction were taken from LUH2 (ref. [68]). To map peat extraction, we converted a global polygon-based peatland map[69] to a 0.5° grid. We used a single set of land-use maps rather than an ensemble, because our approach required us to separate specific land-use classes (for example, irrigated rice and forestry) that are available only from different sources. Moreover, historical land-use maps do not diverge substantially over the period 1800–2000, when most of the drainage occurred.

Reconstruction methodology

Drained area time series hindcasting. We reconstructed time series of the drained area in cropland and forestry by fitting sigmoidal functions using a non-linear optimizer with multiple starting points[70]. A separate sigmoid function was fitted to the national data from 18 countries and land-use type combinations (Supplementary Fig. 14) with sufficient numbers of data points (at least four) in which robust fitting parameters could be achieved (Eufron's pseudo-R^2 median, 0.90; range, 0.24–0.99). Countries with fewer than four data points were not used for fitting because this resulted in unrealistic trajectories (for example, large drainage in 1700, overshoot in 2020). The sigmoidal curve replicates the economic stages of drainage expansion: capacity building, primary then secondary investments and ending with saturation[52,71]. To reconstruct drainage time series in data-poor countries ($0 < n < 4$) we transferred the midpoint and growth rate parameters, but not the upper asymptote, from data-rich exemplary countries within the same continent (Supplementary Fig. 15). This regionalization of the sigmoidal model allowed for generalization of the rate of growth and timing of the inflection point across countries while refitting the upper asymptote to the available data in each new country. To remain conservative, we set the highest reported data point as the upper asymptote of the sigmoidal curve. This upper limit ensures that cumulative mapped losses are constrained by available data. Uncertainty was not propagated from the fitted time series because of the large number of data-sparse countries for which uncertainty is difficult to quantify meaningfully. In the future, with additional metadata compiled from different data sources, a full assessment of the overlap, complementarity and agreement of data sources might be used to account for uncertainty in the national drainage statistics more systematically.

Annual peat extraction rates (t yr^{−1}; Supplementary Fig. 16) were interpolated linearly between data points. We also extrapolated extraction rates back in time, assuming a doubling of extraction rates every decade before our first data point to replicate the rapid growth observed in

data-rich countries (for example, Russia and the United States). Continuous interpolated and extrapolated extraction rates were then used to calculate the cumulative tonnage of dry peat extracted per country since 1700 (Supplementary Fig. 17). Cumulative peat mass extracted was converted to area of peatland drained using a conversion rate of 300,000 t km^{-2} dry peat[272]. Sigmoidal curves were fitted to the cumulative area of peatland extracted to extend the time series to 2020. Then, sigmoid parameters were generalized to countries with available data on extracted peatland area but not on extracted peat mass, following the generalization approach described above.

Data on the area of wetland cultivation were found only for the post-1980 period, preventing us from fitting sigmoidal functions. Instead, we assumed that wetland cultivation has occupied a constant country-specific fraction of cropland area over time. To estimate the area of wetland cultivation over the period 1700–2020 we calculated the fraction of cropland reported as wetland cultivation per country for the period 2000–2020, for which most data were available, and multiplied it by cropland area taken from historical land-use maps (see below). Given the long history of hydrological manipulation and cultivation of several wetland crops (for example, rice and yam), going back to the Neolithic period[73–75], this assumption probably produces conservative estimates of wetland cultivation in 1700 and earlier. Despite its limitations, this assumption is preferable to its alternative—namely, to consider that the area of wetland cultivation in the period 2000–2020 has remained static over time, which would result in a wetland cultivated area in 1700 that is three times higher than that derived from our fractional assumption.

For each of the four land-use drivers above, country-level reconstructed time series were disaggregated to subnational units in 18 countries for which subnational data were available (Supplementary Fig. 4). Because subnational data were generally not available to fit subnational sigmoid functions over sufficiently long periods (Supplementary Fig. 18), we calculated the fraction of each subunit within the national totals for the median year of subnational data. We then used these static fractions to distribute drainage over the period 1700–2020 to subnational units where drainage was prevalent in more recent years. This approach, however, could not capture changes in the subnational distribution of drainage within the same country over time.

Generation of potential wetland cover. To help allocate wetland loss, we generated potential wetland maps representing those areas where wetlands may have formerly existed but are no longer occupied by present-day wetlands. We computed the potential wetland area as the difference between simulated and present-day wetland. Simulated wetland cover is greater than present-day cover in nearly all grid cells, but subtraction can yield some sparsely distributed negative grid cells. Negative values of potential wetland area were set to zero and interpreted as areas where wetlands are underestimated by simulations. We generated 12 potential wetland maps from the cross-combinations of four simulated wetland maps and three present-day wetland maps (Supplementary Fig. 19). Together, this ensemble of 12 potential wetland maps is used to quantify the uncertainty from past and present wetland cover on the estimates of loss.

Mapping drainage from national records. We distributed drained (that is, lost or converted) area (km^2) from national data (L_{data}) within the borders of each country over a 0.5° grid proportionally to the co-occurrence between potential wetland and land-use area. The co-occurence, or overlap of land use and potential wetland, approximates the geographic distribution of land use exposed to wet conditions. Because subgrid cell overlap within the 0.5° grid cells can neither be resolved nor varied across time periods and regions, the overlap assumes random distribution between potential wetland and land use (that is, multiplied grid cell fractions). Grid cell fractions were calculated based on land areas excluding lakes, rivers, ocean and steep slopes

where neither land use nor wetlands are likely to occur[66]. Grid cells in which either no wetland area or no land use existed received no drainage. In the special case of peatland extraction, we prioritized extraction in peatlands near population centres by distributing peat extraction proportionally to $\log_{10}$ of population. Each of the four land-use extents that represent a part of the nationally reported wetland drainage, L_{data} (equation (1)), were mapped individually based on the co-occurence of their respective land use and potential wetland:

$$L_{\mathrm{data}} = L_{\mathrm{cropland}} + L_{\mathrm{forestry}} + L_{\mathrm{peat.extr.}} + L_{\mathrm{wet.cultiv.}} \qquad (1)$$

Modelling losses from other land uses. We estimated wetland area lost to the three land uses without drainage data (that is, irrigated rice, pasture and urban areas), but with available land-use maps, by optimization of three parameters θ_i, one per respective land use i. The calibrated parameters θ_i represent the tendency of each land use to replace natural wetlands, and are weighted in equation (2) by the joint probability F_i of land use and potential wetland fractions $F_{\mathrm{wet.pot}}$. For example, values of θ_i above 1 represent a tendency to preferentially claim land for land use i from wetlands as opposed to uplands. Each parameter θ_i is global, meaning that it applies to all regions and time periods. For example, following equation (2), wetland area lost to irrigated rice is calculated as the product of θ_{rice}, the fraction of the grid cell occupied by rice (F_{rice}), the fraction of potential wetland ($F_{\mathrm{wet.pot}}$) and the grid cell's total land area (A). Total wetland loss (L_{total}) in a grid cell is calculated as the sum of loss from the four land uses based on national data (L_{data}) and the loss from irrigated rice, pasture and urban areas (equation (2)). The three parameters θ_i are fitted through comparison of the reconstruction with regional loss data (Calibrating reconstruction to regional data):

$$L_{\mathrm{total}} = L_{\mathrm{data}} + (\theta_{\mathrm{rice}}F_{\mathrm{rice}} + \theta_{\mathrm{pasture}}F_{\mathrm{pasture}} + \theta_{\mathrm{urban}}F_{\mathrm{urban}})F_{\mathrm{wet.pot}} A \qquad (2)$$

Mapping continuous drainage expansion. At each decadal time step, wetland conversion from the seven land uses was distributed sequentially with the following priority order (first to last): wetland cultivation, irrigated rice, cropland, urban area, pasture, peat extraction, forestry. This order conceptually captures a succession of land use starting with conversions to artificial wetlands, followed by drainage for land uses of high importance and, finally, drainage for land uses with lower economic returns. The ordering of drivers has a minor impact on overall results, and primarily affects the distribution of wetland loss within countries.

At each time step, newly added drained area is distributed across the land uses then the undrained remainder of the land use is updated for the following time step to ensure that land area can be drained once only. The drained area in each grid cell is constrained by total land-use area in the grid cell. Conversely, the potential wetland area is not used as a fixed maximum drainage in a grid cell due to the uncertainty of simulated wetland cover. In some regions the drained area can exceed the potential wetland extent. These upper limits on the distribution of drained areas have caused minor divergences between the total area mapped and original national statistics (Supplementary Table 4).

Estimation of past wetland area. The natural wetland area (W) at time T is calculated by adding the cumulative loss (L) since time t (in decremental order) to the wetland extent in 2020 (W_{2020}), following equation (3):

$$W_T = W_{2020} + \sum_{t=2020}^{T} L_t \qquad (3)$$

Estimation of fractional wetland loss. This approach estimates wetland area by sequential backward addition of wetland loss starting

from the present-day reference, and thus ensures that the reconstruction aligns with present-day wetland maps. The justification for this approach is that present-day wetland maps are more reliable in their depiction of wetland areas than are simulated wetland maps. Hence, we used present-day wetland as the primary source of information for modelling the remaining wetland areas over time, whereas simulated wetland maps have a secondary effect on total losses (Supplementary Fig. 20) by affecting the area converted to the three modelled land uses (irrigated rice, pasture and urban areas). The fraction of wetland lost since time T is calculated by dividing the losses since time T by the total wetland area W_T at time T (equation (4)):

$$P_T = \sum_{t=2020}^{T} L_t / W_T \tag{4}$$

Calibration of reconstruction to regional data. We fitted the parameters θ_i to minimize the residuals of wetland fraction lost between our reconstruction and 121 regional wetland loss records. For each of the 12 potential wetland maps, we ran 5,000 simulations with varying parameters θ_i that were generated using latin hypercube sampling. Values for θ_i were bound between 10^{-3} and 30 based on iteratively narrowing the range containing optimal parameters. Residuals of fraction wetland loss were weighted by region area, to ensure that reconstruction reproduced the major regions of loss. Because simulations of parameters θ_i did not all reliably converge to an optimal set of three values, we estimated the average and range of parameter values from the 100 best simulations per potential wetland map. Optimization equifinality is probably caused by internal model constraints and thresholds (for example, drained area limited by land availability) that are insensitive to the values of parameters θ_i.

The averaged best θ_i parameter ranges (Supplementary Fig. 21) across the 12 simulations were $\theta_{rice} = 9.07–12.9$, $\theta_{pasture} = 11.3–15.6$ and $\theta_{urban} = 0.19–1.23$. The wide range of $\theta_{pasture}$ is caused by an added constraint limiting pasture drainage from exceeding the percentage of cropland drained in the same country and time period. This constraint is based on the understanding that economic investment toward drainage is generally first expended on cultivated land because pastures can be exploited for livestock grazing under wet conditions. We introduced this constraint to prevent pasture drainage from growing to an unreasonably large area, and from compensating for gaps in drainage data. This constraint is the reason why the best reconstruction members tend to be on the high end of the parameter range, because $\theta_{pasture}$ values beyond the pasture-cropland constraint have ceased to influence mapped pasture drainage. The high fitted θ_{rice} value suggests that natural wetlands were preferentially used to claim land for irrigated rice culture and reflect the large extensive rice cultivation of China in the twentieth century, from which nearly one-third of regional data originate. This reliance on recent regional data may exaggerate conversion to rice in the decades after 1700. Whereas we treat irrigated rice as a land use alongside others, other scenarios could be tested in the future, such as the assumption that all wet rice is first located in wetland areas and starts to expand upland only once wetland areas are exhausted. Wetland losses to urban areas are comparatively low, which can be explained by our inclusion of only direct wetland conversion (that is, wetland to urban), whereas many urban areas may be located in former wetlands that were first converted to cropland.

The parameters θ_i varied only moderately among the 12 potential wetland simulations. Some potential wetland maps generated better agreement with regional wetland loss data: in particular, WAD2M was present in the top four scenarios. Among simulated wetland maps, the LPJ-wsl map led to higher regional agreement because its wetland coverage was more widespread, which allowed it to distribute loss in areas where other maps estimated no wetland area. As a result, the reconstruction with highest agreement using the WAD2M present-day wetland map and LPJ-wsl simulated wetland is shown in Figs. 1–3 (and see Supplementary Fig. 22 for country timelines).

Uncertainty assessment and validation

We quantified the uncertainty of global wetland losses originating from three primary sources: (1) parameters θ_i, (2) simulated wetland maps and (3) present-day wetland maps. To isolate the uncertainty from each of these three components, we computed wetland losses from the 200 simulations with parameters θ_i achieving the highest agreement with regional data for each of the 12 potential wetland maps. The range of losses from this ensemble is shown in Fig. 1a. Holding other factors constant, the range of wetland loss percentage from the best-fit reconstructions is 0.7% across the the three different present-day wetland areas; 1.7% from the four simulated wetland areas; 2.5% from their combination constituting the ensemble of 12 potential wetland cover; and 3.9% from the θ_i parameter uncertainty (2.5th and 97.5th percentiles of parameters). This attribution underlines the uncertainty related to the modelled land uses (irrigated rice, pasture and urban areas), greater than the contribution of potential wetland to the overall uncertainty range of 7.1%. The range of uncertainty from the best-fit reconstruction across the different present and simulated wetland maps illustrates the importance of the fitting process in narrowing this range. The fact that best-fit reconstructions are near the upper bound of the uncertainty range also suggests that our reconstruction is probably conservative.

To evaluate the contribution of the three modelled land uses (irrigated rice, pasture and urban areas), we compared wetland loss reconstructed from only the four land uses with national statistics to the regional data (that is, $\theta_{rice} = \theta_{pasture} = \theta_{urban} = 0$). With this reconstruction only from national statistics, we find moderate agreement ($R^2 = 0.55–0.62$ across the ensemble of 12 reconstructions, $n = 121$) and an overall underestimation of percentage loss (average bias −18.0 to −25.5%; Supplementary Fig. 23). This bias indicates that the remaining disagreement is partially due to unaccounted drivers of wetland loss, and provides justification for their inclusion through modelling. Our ability to capture regional differences in drainage intensity of irrigated rice, pasture and urban areas could be improved by applying a modelling scheme with varying parameters θ_i across regions and time periods. However, data availability does not currently allow for this.

Nevertheless, even with the inclusion of the three modelled land uses, large disagreements in individual regions can arise from various causes. For instance, gaps in drainage data lead to underestimation of wetland losses in some areas (for example, Lake Chad) whereas losses in arid regions (for example, Xinjiang in China) are underestimated because wetland simulations do not predict the former riverine wetlands, leading to the distribution of wetland drainage telsewhere. It is also possible that the independent literature estimates include additional drivers of loss that were not included in our reconstruction, possibly contributing to the negative bias in our results.

Finally, to evaluate the capacity of our calibrated model to generalize from a subset of the 121 regional estimates to new regions (that is, providing a more representative accuracy over regions not covered by the regional data), we conducted a cross-validation exercise in which 90% of the data were used to fit the parameters θ_i, and compared results with the 10% of withheld data for an independent accuracy estimate. The mapping and parameter-fitting process was identical to the full reconstruction. Repeating this process across ten randomly sampled folds resulted in a training root mean squared error of 80.1 (range 72.0–88.5, $n = 108$) and validation root mean squared error of 82.0 (range 55.5–110.4, $n = 12$). This error gap suggests that the parameters θ_i generalize relatively well to new regions, but that the geographic clustering of regional loss data can lead to unstable results when large key regions are withheld from training. Conversely, small regions with high losses (for example, Lake Urmia in Iran) that are difficult to capture by the coarse resolution of our approach are adversely affecting model generalization to other regions.

Regional summary of wetland loss

We summarized wetland area change across countries, river basins and peatland regions. Hotspots of loss within and across countries were defined as contiguous areas with over 50% wetland loss since 1700. We summarized losses by river basins with the basin outlines from the ISLSCP river network[76]. Peatland-rich regions were delineated by applying a 20% area threshold to the PEATMAP product[69], gridded at 0.5° resolution. Global and regional peatland losses were estimated by assuming that the share of peatland versus other wetland loss is in proportion to their present share of coverage in each grid cell. This approach leads us to estimate that peatlands account for 15% of the losses from all seven land uses. However, this percentage is probably an underestimate because areas where peatlands were extirpated are overlooked (see Supplementary Fig. 7 for peatland distribution).

Usage notes

Drainage and wetland extent were mapped at coarse resolution, which may be inaccurate over small regions and short time periods. Use of our reconstructed maps should thus be reserved for applications at the continental to global scales. Available regional maps of drainage and wetland distribution that we were unable to integrate into our globally applicable method should be presumed more reliable locally and preferred for regional-scale studies.

Data availability

Data for national and subnational statistics of drained or converted areas, regional wetland percentage loss estimates, and gridded reconstruction of drained area per land use and cumulative—as well as natural wetland area—are available at https://doi.org/10.5281/zenodo.7293597.

Code availability

The scripts used to process input data, model and calibrate the wetland loss reconstruction, and produce the figures are publicly available at https://github.com/etiennefluetchouinard/wetland-loss-reconstruction.

44. de Zeeuw, J. W. Peat and the Dutch golden age. The historical meaning of energy-attainability. *A. A. G. Bijdr.* **21**, 3–31 (1978).
45. Woodward, C., Shulmeister, J., Larsen, J., Jacobsen, G. E. & Zawadzki, A. The hydrological legacy of deforestation on global wetlands. *Science* **346**, 844–847 (2014).
46. Feick, S., Siebert, S. & Döll, P. *A Digital Global Map of Artificially Drained Agricultural Areas* (Johann Wolfgang Goethe-Universität Frankfurt am Main, 2005); https://www.uni-frankfurt.de/45217762/FHP_04_Feick_et_al_2005.pdf.
47. *Irrigation and Drainage in the World – A Global Review* Vols I–III (International Commission on Irrigation & Drainage, 1982).
48. *FAOSTAT* (Food and Agriculture Organization of the United Nations, accessed 21 October 2021); https://www.fao.org/faostat/en/.
49. McCorvie, M. R. & Lant, C. L. Drainage district formation and the loss of Midwestern wetlands, 1850–1930. *Agric. Hist.* **67**, 13–39 (1993).
50. AQUASTAT (Food and Agriculture Organization of the United Nations, accessed 17 August 2018); https://www.fao.org/aquastat/en/.
51. Kearns, K. C. Development of the Irish peat fuel industry. *Am. J. Econ. Sociol.* **37**, 179–193 (1978).
52. Schultz, B., Zimmer, D. & Vlotman, W. F. Drainage under increasing and changing requirements. *Irrig. Drain. Syst.* **56**, S3–S22 (2007).
53. Niu, Z. et al. Mapping wetland changes in China between 1978 and 2008. *Chin. Sci. Bull.* **57**, 2813–2823 (2012).
54. Dahl, T. E. *Wetlands Losses in the United States 1780's to 1980's: Report to Congress* (US Department of Energy, 1990).
55. Zhang, Z., Fluet-Chouinard, E. & Jensen, K. Development of the global dataset of Wetland Area and Dynamics for Methane Modeling (WAD2M). *Earth Syst. Sci. Data* **13**, 2001–2023 (2021).
56. Prigent, C., Jimenez, C. & Bousquet, P. Satellite-derived global surface water extent and dynamics over the last 25 years (GIEMS-2). *J. Geophys. Res. Atmos.* **125**, e2019JD030711 (2020).
57. Lehner, B. & Döll, P. Development and validation of a global database of lakes, reservoirs and wetlands. *J. Hydrol.* **296**, 1–22 (2004).
58. Pekel, J.-F., Cottam, A., Gorelick, N. & Belward, A. S. High-resolution mapping of global surface water and its long-term changes. *Nature* **540**, 418–422 (2016).
59. Carroll, M. L., Townshend, J. R., DiMiceli, C. M., Noojipady, P. & Sohlberg, R. A. A new global raster water mask at 250 m resolution. *Int. J. Digit. Earth* **2**, 291–308 (2009).
60. Portmann, F. T., Siebert, S. & Döll, P. MIRCA2000–global monthly irrigated and rainfed crop areas around the year 2000: a new high-resolution data set for agricultural and hydrological modeling. *Global Biogeochem. Cycles* **24**, March 2010 (2010).
61. Hugelius, G. et al. The Northern Circumpolar Soil Carbon Database: spatially distributed datasets of soil coverage and soil carbon storage in the northern permafrost regions. *Earth Syst. Sci. Data* **5**, 3–13 (2013).
62. Gumbricht, T. et al. An expert system model for mapping tropical wetlands and peatlands reveals South America as the largest contributor. *Glob. Chang. Biol.* **23**, 3581–3599 (2017).
63. Zhang, Z., Zimmermann, N. E., Kaplan, J. O. & Poulter, B. Modeling spatiotemporal dynamics of global wetlands: comprehensive evaluation of a new sub-grid TOPMODEL parameterization and uncertainties. *Biogeosciences* **13**, 1387–1408 (2016).
64. Beven, K. J. & Kirkby, M. J. A physically based, variable contributing area model of basin hydrology. *Hydrol. Sci. Bull.* **24**, 43–69 (1979).
65. Wania, R. et al. Present state of global wetland extent and wetland methane modelling: methodology of a model inter-comparison project (WETCHIMP). *Geosci. Model Dev.* **6**, 617–641 (2013).
66. Goldewijk, K. K., Beusen, A., Doelman, J. & Stehfest, E. Anthropogenic land use estimates for the Holocene – HYDE 3.2. *Earth Syst. Sci. Data* **9**, 927–953 (2017).
67. Goldewijk, K. K., Beusen, A., Van Drecht, G. & De Vos, M. The HYDE 3.1 spatially explicit database of human-induced global land-use change over the past 12,000 years. *Global Ecol. Biogeogr.* **20**, 73–86 (2011).
68. Hurtt, G. C. et al. Harmonization of global land use change and management for the period 850–2100 (LUH2) for CMIP6. *Geosci. Model Dev.* **13**, 5425–5464 (2020).
69. Xu, J., Morris, P. J., Liu, J. & Holden, J. PEATMAP: refining estimates of global peatland distribution based on a meta-analysis. *Catena* **160**, 134–140 (2018).
70. Padfield, D. & Matheson, D. P. A. nls.multstart: Robust non-linear regression using AIC scores. *R Project* https://mran.microsoft.com/snapshot/2021-08-04/web/packages/nls.multstart/index.html (2020).
71. Smedema, L. K., Abdel-Dayem, S. & Ochs, W. J. Drainage and agricultural development. *Irrig. Drain. Syst.* **14**, 223–235 (2000).
72. Murphy, F., Devlin, G. & McDonnell, K. Benchmarking environmental impacts of peat use for electricity generation in Ireland—a life cycle assessment. *Sustain. Sci. Pract. Policy* **7**, 6376–6393 (2015).
73. Denham, T. Archaeological evidence for mid-Holocene agriculture in the interior of Papua New Guinea: a critical review. *Archaeol. Oceania* **38**, 159–176 (2003).
74. Fuller, D. Q. & Qin, L. Water management and labour in the origins and dispersal of Asian rice. *World Archaeol.* **41**, 88–111 (2009).
75. Bellwood, P. The checkered prehistory of rice movement southwards as a domesticated cereal—from the Yangzi to the Equator. *Rice* **4**, 93–103 (2011).
76. Vörösmarty, C. J. & Fekete, B. ISLSCP II river routing data (STN-30p). *ORNL DAAC* https://daac.ornl.gov/cgi-bin/dsviewer.pl?ds_id=1005 (2011).

Author contributions E.F.-C. conceived and designed the study, with input from J.R.M., B.D.S., A.M., Z.Z., B.P., P.B.M. and R.B.J. E.F.-C., S.S. and T.M. compiled drainage data. Wetland area data were provided by Z.Z., B.D.S., J.R.M. and B.L. Land-use data were provided by K.K.G. E.F.-C. developed the model calibration, with advice from B.D.S., J.M. and Z.Z. E.F.-C. wrote the manuscript with input from P.B.M., and all authors edited the final version.